

Shahid Chamran
University of AhvazIranian Association of
Electrical and Electronics
Engineers

Journal of Applied Research in Electrical Engineering



E-ISSN: 2783-2864

P-ISSN: 2717-414X

Homepage: <https://jaree.scu.ac.ir/>

Research Article

Efficient Responding to Demand and Robust Voltage Control of an Islanded DC Microgrid Under Variations in Load and Supply

Sajed Derakhshani Pour ^{1,2} , and Reza Eslami ^{2*} 

¹ Department of Energy, Polytechnic University of Milan, Milan, Italy

² Department of Electrical Engineering, Sahand University of Technology, Tabriz, Iran

* Corresponding Author: eslami@sut.ac.ir

Abstract: In the last few years, there has been growing attention to isolated DC microgrids (MGs) with robust voltage control and efficient responding to demand in the face of fluctuating demands and supply amounts. This attention is due to significant voltage mismatches originated from the sudden transitions of the load demand and the active power of the supplies such as photovoltaic (PV) systems. To address these goals, a novel nonlinear robust voltage control strategy with a cascaded design consisting of proportional-integral (PI) and sliding mode control (SMC) techniques is developed in this research for the battery energy storage system (BESS). Additionally, this research considers a fuel cell as another power supply in addition to a solar PV system. For maximum power point tracking (MPPT) of the PV system, a novel backstepping sliding mode control (BSMC) technique is developed as well. The effective functioning of the suggested cascaded control strategy is examined using MATLAB/Simulink. The outcomes of the simulation represent the effectiveness of the proposed approach in robustly regulating the voltage level of the DC link at 50 V with small deviations in tracking, and quick reaction to fluctuations in both demand and supply sides, as well as guaranteeing an evenly-distributed responding to demand fluctuations from the DC MG.

Keywords: DC microgrid, cascaded robust voltage control, maximum power point tracking, battery energy storage system, backstepping sliding mode control, renewable energy sources

Article history

Received 08 January 2024; Revised 29 March 2024; Accepted 18 April 2024; Published online October 9, 2024.

© 2024 Published by Shahid Chamran University of Ahvaz & Iranian Association of Electrical and Electronics Engineers (IAEEE)

How to cite this article

S. Derakhshani Pour, and R. Eslami, "Efficient Responding to Demand and Robust Voltage Control of an Islanded DC Microgrid Under Variations in Load and Supply," *J. Appl. Res. Electr. Eng.*, Vol. 3, No. 1, pp. 51-63, 2024. DOI:

[10.22055/jaree.2024.45776.1100](https://doi.org/10.22055/jaree.2024.45776.1100)



1. INTRODUCTION

1.1. Motivations

The global shift away from conventional energy sources, notably fossil fuels, and toward renewable energy sources (RESs) such as solar PV systems keeps on gaining traction. This trend is being motivated by growing awareness of the considerable disadvantages connected with the use of fossil fuels. These negatives include the discharge of greenhouse gases and contaminants, the gradual dwindling of limited resources, which leads to crises in the energy sector, financial obligations, and the deterioration of current energy systems' functionality. Deployment of RESs, notably PV systems, is a possible approach for reducing the environmental effect of conventional supplies of energy. Nevertheless, the intermittent characteristic of RESs must be addressed. Solar

energy generation, for example, is affected by the climate and sunlight accessibility. To tackle this constraint and provide a continuous and reliable energy supply, rising attention is being placed on combining RESs with BESSs within MG. The power balance between the generating and consumption sides is maintained by adding BESSs into MG. BESSs are critical in storing surplus energy created during maximum generation intervals and providing it during weak or zero power generation time frames. This coordination improves the MG's reliability by optimizing power dispatch. By effectively controlling the flow of power, the MG becomes healthier and stable, lowering the danger of disturbances. Furthermore, concerted attempts in power sharing among various domains enable greater RES use while mitigating the effect of their intermittent behavior. This implies that variations in renewable energy production, such as those induced by shifts in weather, can be minimized

through concerted activities, resulting in a more seamless integration of RES into the grid structure [1, 2]. As a fundamental configuration, energy communities (ECs) are defined as a collection of demands and supplies that exchange energy on a local distribution grid [3]. ECs are not considered as islanded MGs. MGs are responsive electric power systems that can be divided into DC and AC MGs. DC MGs have various benefits over AC MGs [4, 5, 6]. The absence of frequency and reactive power characteristics is a considerable benefit. Maintaining a constant frequency and regulating reactive power in AC systems are challenging and need extra control techniques. DC MGs eliminate the requirement for frequency synchronization and reactive power control by running on a consistent voltage range. Additionally, DC MGs provide improved and more precise system operation. The lack of frequency variations enables greater control over power flow and voltage values. This improved degree of control leads to a more robust and rapid energy delivery system, which is critical for managing current power grid needs [7]. The great reliability of DC MGs is a further significant benefit. The DC design's straightforwardness, with a fewer number of elements and less complexity, leads to better system reliability. This is especially beneficial in situations where grid resilience and robustness are required, such as critical facilities and distant sites. Furthermore, DC MGs enable greener solutions for preserving the environment. The removal of some power conversion procedures, as well as the intrinsic efficiency of DC transmission, decreases energy losses and has minimal effect on the ecosystem. This is consistent with the global quest for renewable and environmentally friendly energy options [8]. Fig. 1 represents the architectural framework of the suggested DC MG design. This arrangement is a simplified and effective structure that combines multiple components ideally to provide secure and renewable energy delivery. The PV system, a critical RES, sits at the heart of the entire framework. A DC-DC step-up converter appropriately connects the PV array to the DC link. This converter is an important component of the system because it allows for the effective transformation of the produced DC voltage from the PV array to the appropriate useful voltage of the DC bus. This procedure is critical for guaranteeing the energy generated by the solar panels is adequately absorbed and incorporated into the MG. Furthermore, a fuel cell is considered as the second power supply to help the PV system in properly meeting the load demand. This power supply source is linked to the DC bus through a unidirectional DC-DC converter which is managed by SMC. Finally, the proposed DC MG includes a BESS to improve versatility and robustness. A DC-DC bidirectional converter properly connects the BESS to the DC link. This reversible converter manages the two-way flow of power between the DC link and the BESS. The bidirectional converter facilitates the storing of surplus energy in the BESS during periods of extra production. When the energy request exceeds the immediate supplies of the PV system and fuel cell, the converter permits the transfer of stored energy from the BESS, assuring an uninterrupted and reliable power supply to the MG. The proposed layout has many benefits. The integration of the PV array, fuel cell and BESS via specialized DC-DC converters enables a more straightforward and regulated energy flow, reducing energy losses and improving overall system efficiency. Furthermore, the BESS-connected converter's bidirectional capabilities provide a layer of flexibility, allowing the MG to rapidly respond to changes in both consumption and supply sides,

which lead to various voltage drops and spikes. These voltage mismatches are addressed and suppressed by the proposed control algorithm.

1.2. Literature Review

In recent years, the robust voltage control and equal responding to demand of isolated DC MGs including PV, BESS, and other power supplies have arisen as major focuses of academic inquiry. The necessity to overcome the issues provided by fluctuating loads and supply variations is driving growing curiosity in these areas. Isolated DC MGs, which are meant to function independently of the main utility grid, must deal with unpredictable and unexpected situations, necessitating complex control systems for maximum efficiency. Robust voltage control is an essential part of this solution. Voltage stability, an important feature of MG functioning, is critical to guaranteeing the MG system's steady and reliable performance, especially in the face of unpredictable variations in both demand and supply. As demand varies during the day, and RESs bring unpredictability into the supply combination, voltage stability becomes critical. Voltage stability refers to the MG's capability to preserve proper voltage levels within accepted boundaries, avoiding voltage spikes or undervoltages that could cause malfunctions or operational disturbances. In the face of shifting consumption patterns and intermittent renewable energy production, enhanced monitoring, control, and administration solutions are critical for dynamically altering voltage levels and optimizing performance to meet the MG's developing requirements. Researchers have been actively investigating novel regulation strategies for maintaining a steady voltage profile, hence improving the resilience of DC MG [9, 10]. At the same time, demand response is the process of regulating and altering customer usage of energy in reaction to evolving circumstances inside the MG. Finding a harmonic balance between generation and demand is critical for grid stability and avoiding instabilities that can contribute to power outages. Consequently, a broad range of control systems for MGs have been presented in the literature, including droop control, SMC, droop-SMC, fuzzy logic, artificial intelligence (AI), and model predictive control (MPC) strategies. An adaptive droop control technique for DC MG has been defined in [11], with the main goal of successfully handling voltage control issues and guaranteeing an equal flow of current within the DC MG structure. By dynamically adjusting droop characteristics, this approach enhances voltage stability and promotes a balanced flow of current, thereby optimizing the performance and reliability of DC microgrid systems. [12] introduces a unique converter control approach based on a configurable variable droop coefficient. The fundamental goal of this strategy is to maintain voltage stability when there are considerable and rapid variations in power inside the system. [13] makes a substantial addition by presenting a unique adaptive droop control approach specially developed to support an integral feed-forward SMC within the PV-BESS DC MG framework to considerably increase each BESS converter's voltage response speed. [14] suggests integrating universal droop control with SMC to provide distributed energy resource (DER) integration and power-sharing management for the DC MG, therefore solving the DC MG's power stability. [15] advances sustainable energy

integration by utilizing SMC and PWM pulses to enhance PV power production while maintaining DC voltage stability in an integrated system comprised of PV, wind, and BESS. In order to indicate the operational advantage of DC MG, [16] develops an SMC with an integrated design and compares it to a simple PI control method. This comparative study highlights the enhanced effectiveness of operation and performance benefits given by the SMC in DC MG structures. In [17], the contributors have proposed an adaptive SMC particularly designed for dc-dc step-up converters, which is systematically implemented within the framework of PV-Wind-BESS-EV DC MG that serves CPLs in order to guarantee the maintaining adequate stability margins, especially when encountered with significant and sudden changes in load demand. In [18], an important breakthrough in control methods is proposed by the introduction of an adaptive fuzzy integrated fractional order controller that is particularly developed for a DC MG consisting of a hybrid energy storage system (HESS) to improve DC link voltage regulation, addressing and eliminating imbalances between consumption and supply within the MG. The artificial neural networks (ANNs) control approach is presented in [19] as a particular type of Artificial Intelligence (AI) for a DC MG consisting of DERs and BESS in order to enable efficient control of power converters while preserving efficiency, thus enhancing the general adaptability of the system and ensuring that the DC link voltage continues to be inside the admitted boundaries, improving the system's stability and reliability. [20] entails a decentralized model predictive control (DMPC) structure aimed at preserving voltage stability and equal power dispatch within a DC MG characterized by constant power loads (CPLs). This approach contributes to improve system performance and reliability by dynamically controlling voltage levels and guaranteeing equal power sharing across the grid. [21] also compares a unique model predictive control (MPC) approach and linear control strategy in view of successfully managing the DC link voltage level of a DC-DC step-up converter while also preserving the stability of the DC MG in the face of dynamic load behavior.

1.2.1. Gaps and Contributions

Given the information presented thus far, it is undeniable that there are significant gaps in the existing corpus of literature. In [11, 12, 13, 14] obtaining accurate control and proper power sharing in droop control schemes can be difficult, resulting in voltage error and unequal supply usage, particularly in systems with fluctuating loads and operating cases. Droop control techniques are also easily affected by modifications in system variables. The changes in such variables can have an impact on the precision of droop calculations. These solutions have generally been intended for unidirectional power flow, which may restrict their usefulness in bidirectional power flow structures, particularly those that incorporate RESs and BESSs. Finally, these systems may have response time restrictions, especially in circumstances requiring quick and exact modifications. Although using a single SMC technique in [15, 16, 17] provides robust and rapid functionality in the face of uncertainty, it suffers from chattering issues due to high-frequency fluctuations or fast switching of duty cycle near the sliding surface, which can cause probable

steady-state challenges and undesired damage to the materials in physical structures. The fuzzy logic control strategy, which is used in [18], is based on cognitive principles and fuzzy logic sets, which leads to issues in the exact modeling of complicated system characteristics. Precise fuzzy principles can be challenging to expand, especially in nonlinear systems that have time-dependent dynamics. These controllers may have difficulty adapting to abrupt alterations in system characteristics. They are built to cope with slowly shifting conditions and may show shortcomings in quickly shifting surroundings. More sophisticated control approaches may be necessary in some circumstances for successful control in extremely nonlinear or unpredictable cases. In [19], knowing the network's underlying functions and procedures for making decisions might be difficult, resulting in an absence of clarity. Furthermore, the network's functionality is heavily impacted by the type of training data. In cases when the data is restricted or prejudiced, the ANN might be unable to generalize effectively to previously encountered instances. As a result, ANNs may experience difficulties responding to fast-changing systems. MPC strategies in [20, 21] are computationally complicated and take a significant amount of computing time and money to implement due to the large uncertainties in the modeling of the system, which may restrict applications that operate in real-time, especially in systems that demand quick reactions. Additionally, MPC only depends on the precise model of the system for forecasting, and any differences between the model and the real system performance might result in poor functionality. As a result, MPC is affected by model uncertainty, variable changes, and disruptions.

According to the gaps found in the existing literature above, the following are the goals and contributions of this research:

- I. A novel nonlinear robust control strategy, which combines the advantages of PI control with SMC, is introduced for a PV-BESS-fuel cell DC MG with the primary goals of assuring robust DC link voltage regulation and providing evenly-distributed response to fluctuating load demands and solar exposures.
- II. A BSMC approach, whose basic concept is the utilization of MPPT to maximize peak power harvesting from solar PV systems, is used to improve the efficiency of solar output power extraction by continuously and automatically controlling the operating point of the PV system to coincide with the MPP.
- III. In comparison to other control approaches, the suggested method notably has lower DC link voltage oscillations, more robust functioning, more rapid dynamic responsiveness, and less chattering influences. These distinguishing traits contribute to the suggested control approach's effectiveness.

1.3. Paper Arrangement

The remainder of the paper is organized in the following order: The suggested DC MG concept is described in section 2. Section 3 presents formulations of the suggested control technique. Section 4 depicts simulation findings and scenarios. Section 5 finally concludes the paper.

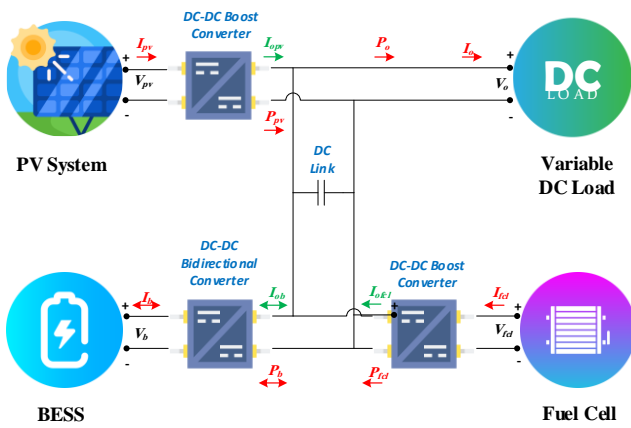


Fig. 1: DC MG structure

2. MODEL DESCRIPTION

2.1. PV Array

Solar PV systems stand out as a superior alternative to standard DC MG power sources when it comes to power supply possibilities. The capability of PV systems to generate zero greenhouse gases contributes greatly to ecological sustainability while at the same time lowering power production costs. Solar irradiation and cell temperature are important parameters affecting the efficiency of PV systems since they directly affect the output power of the PV panels. A systematic strategy is used to maximize the system's performance. The solar array is smoothly incorporated into the DC link via a DC-DC step-up converter, which is an important component in guaranteeing an optimized power supply to satisfy the load needs. The requirement to run at the maximum power based on the P-V curve is an essential concept guiding the operation of solar PV arrays. This exact position on the curve ensures that the panels generate the highest amount of power feasible. The MPP-based BSMC is used to attain this level of accuracy in operation. This complex control system successfully tracks and adjusts for variations in the irradiation amount, ensuring that the PV array runs at its highest productivity point constantly. The PV module under discussion, the KC200GH-2P type, has 54 series-connected cells, each of which contributes to its total electrical properties. Table 1 provides a complete summary of the electrical characteristics, providing an in-depth look into the module's parameters and performance characteristics. These metrics include a variety of key data points, such as voltage, current, and power levels and provide a thorough insight of the module's behavior under varied situations.

Table 1: The electrical specifications of the PV panel

Parameters	Values
MPP voltage V_{mpp}	26.6 [V]
MPP current I_{mpp}	7.55 [A]
Maximum power P_{mpp}	200 [W]
Short circuit current I_{sc}	8.21 [A]
Open circuit voltage V_{oc}	32.9 [V]
Temperature coefficient of SC current K_{sc}	0.00479
Diode ideality factor n	1.8
Cell temperature T	25 [°C]

2.2. Fuel Cell

A fuel cell, by incorporating an additional power source into the system, plays a supporting function in improving the ability to respond of the PV system to variable load demands. The fuel cell, which operates at a constant power output of 100 W, is purposefully utilized to offer an extra energy supply, guaranteeing a steady and reliable power supply to satisfy the dynamic demands of the load. A unidirectional DC-DC boost converter is the vital component developed for effectively carrying energy from the fuel cell to the system, facilitating the connection between the fuel cell and the DC link. SMC approach is used to regulate this converter, which is a robust and adaptive control method noted for its capability to tolerate inconsistencies and disturbances in the system. This adaptive control method enables accurate power output modification, guaranteeing that the fuel cell's extra energy instinctively supports the PV system's reaction to variable load demands. The integrated functioning of those parts not only improves the total reliability of the power production but also maximizes the use of RESs, demonstrating a comprehensive method for greener and responsive power systems.

2.3. Battery Energy Storage System

A BESS performs a crucial act in properly regulating the power imbalance that frequently occurs between supply and consumption inside a DC MG. A bidirectional DC-DC converter is used to provide a smooth link between the BESS and the DC link. This converter acts as an important interface, facilitating the regulated flow of electrical power between the BESS and the MG, as well as charging and discharging activities as necessary. The deployment of a PI-SMC strategy can be a complex and versatile control method designed to assure the DC MG's efficient and steady performance. This controller is critical in coordinating the BESS's charging and discharging operations, dynamically answering to changes in power demand and generation. This multidimensional strategy for BESS control not only tackles power discrepancy issues but also improves the overall reliability and efficiency of the DC MG, demonstrating the need for cutting-edge control tactics in present-day energy management. By synchronizing the power flow with the system's changing needs, the PI-SMC controller helps the DC MG's proper and balanced functioning by efficiently managing the following two operation phases:

Charging mode: The BESS plays a critical role during charging in effectively handling the extra power supplied by both the PV system and the fuel cell. This occurs when the needed output power to fulfill the demanded power is less than the total amount of power provided by the solar PV and the fuel cell. The BESS works as a repository for unused energy during this period, successfully gathering extra power that would otherwise go wasted. The energy storage system provides for the most efficient use of produced power, reducing waste and assuring a long-term solution to energy management. This mode is critical for system balance since it facilitates the storing of more energy during periods of ample supply, allowing the BESS to satisfy load

demand effortlessly in later time frames when generation may be inadequate.

Discharging mode: In this phase, a scenario occurs in which one of the suppliers is unable to entirely match the desired load power. In such cases, the system easily switches to utilizing the stored energy of the BESS, commencing a discharge operation to compensate for the shortage in total power generated by the PV array and the fuel cell. This mode is critical for providing an uninterrupted power supply, particularly when fluctuating solar irradiation or unanticipated changes in load demand influence the capability of the PV array and the fuel cell to produce adequate power on their own. The BESS acts as a dependable backup, delivering stored energy to meet the disparity between the total generation and the needed load power.

3. CONTROL STRATEGY FORMULATION

3.1. MPPT Control

A robust MPP-based BSMC control algorithm has been developed to enhance the productivity of the PV system. To guarantee maximum output power, the BSMC algorithm has two meticulously built control loops. The first control loop, dubbed the MPP block, takes advantage of both the PV voltage and the PV current. This block is in charge of determining the maximum point of the PV system and then creating the MPP voltage. In the second control loop, the MPP voltage acts as a critical reference value [22]. In the BSMC algorithm, the secondary control loop is in charge of producing the control signal that governs overall system behaviour. As shown in Fig. 2, this is accomplished by analyzing a variety of input values, comprising the voltage and current values of the PV, MPP reference voltage, inductor current, and output voltage. Each of these characteristics is critical in selecting the best operating conditions for the PV system. This dual-loop control technique enables meticulous and continuous performance improvement of the PV system. The system can adjust to shifting climatic circumstances and fluctuations in solar input by utilizing the MPP-based BSMC, guaranteeing that the PV system runs at the highest possible efficiency. The complicated interaction of these control loops and taking into account many factors result in the overall control system's resilient and adaptable behaviour, improving the PV system's reliability and output in the presence of various operating conditions.

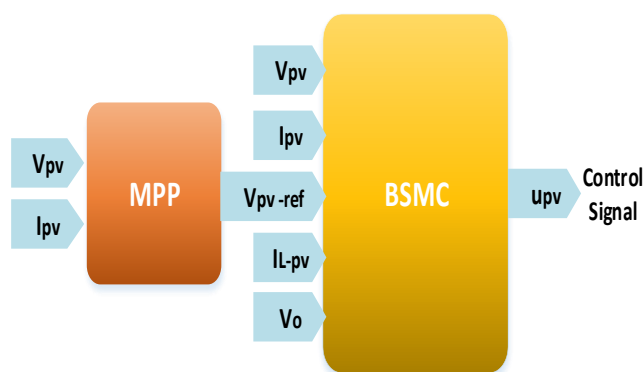


Fig. 2: MPP tracking strategy

$$I_{pv} = N_p \cdot I_{ph} - N_p \cdot I_{sat} \left[\exp\left(\frac{V_{pv}}{\alpha N_s}\right) - 1 \right] \quad (1)$$

where the quantity of cells linked in parallel and series are represented as N_p and N_s respectively. The cells arranged in parallel enhance current output, whereas the cells arranged in series boost voltage potential. To obtain the necessary voltage and current rates, the PV arrays frequently use a mixture of parallel and series connections. Moreover, I_{pv} depicts the electric current produced by PV cells as a result of solar exposure that falls on them. Factors such as sun irradiation and cell temperature impact this number. Additionally, V_{pv} indicates the electrical potential differential between the solar cell terminals. The voltage produced is determined by the solar cell's properties as well as its operational circumstances. Finally γ shows a fixed value as the following equation:

$$\gamma = \frac{n \cdot T \cdot k_B}{q} \quad (2)$$

where $q = 1.6 \times 10^{-19}$ describes the amount of an electron's electrical charge, which is essential in comprehending electric currents and the functioning of semiconductor technologies. Also, n symbolizes the ideality factor of the P-N junction. This factor, also known as the diode ideality factor, is a metric that compensates for departures from a perfect operation of a diode. It takes into account recombination and other non-ideal phenomena. Furthermore, the Boltzmann constant is displayed as $k_B = 1.3805 \times 10^{-23}$, which is important in statistical mechanics and is utilized to connect the average kinetic energy of molecules in gas form to their temperature. Eventually T reflects the cell's temperature in absolute terms, which is a key variable in semiconductor physics because it affects the energy flow of charge transporters, which determines the general behavior of semiconductor technologies.

$$I_{sat} = I_{satr} \left(\frac{T}{T_r}\right)^3 \exp\left(\frac{E_g \cdot T}{\gamma} \left[\frac{1}{T_r} - \frac{1}{T}\right]\right) \quad (3)$$

where I_{sat} points out the cell's reverse bias saturation current, which quantifies the leakage current while the system is in reverse bias mode. In other words, it measures the movement of minority carriers throughout the dwindling zone. $E_g = 1.1$ reflects the semiconductor's energy gap which is the least amount of energy necessary for an electron to pass from the band known as the valence to the conduction region to transmit electricity. The reverse bias saturation current at the reference temperature T_r is indicated as I_{satr} which is given as the following equation[22]:

$$I_{satr} = \frac{I_{sc}}{\exp\left(\frac{V_{oc}}{\gamma \cdot N_s}\right) - 1} \quad (4)$$

where I_{sc} represents the short circuit current which is used to calculate the greatest amount of current that a circuit can supply when it is closed with no resistance. Also, V_{oc} exhibits the open circuit voltage which offers information on the potential gap across the circuit when no current is flowing. The photocurrent I_{ph} , which is the electric current produced by the capture of solar exposure in

a PV cell, is dependent on the cell temperature and sun irradiances by the following expression [22]:

$$I_{ph} = 10^{-3} \cdot E [I_{sc} + K_{sc}(T - T_r)] \quad (5)$$

where E denotes the amount of solar exposure that comes from the sun per unit area. Solar exposure shifts which are impacted by factors like as geographic position, time of day, and climate, have a direct effect on the quantity of energy a PV system can generate. Additionally, K_{sc} depicts the temperature coefficient of short circuit current which measures the effect of temperature fluctuations on a solar cell's short-circuit current. The solar cell functionality may suffer as temperatures increase, and short circuit current drops. Thus, PV output power P_{pv} can be obtained as follows by taking (1) into account:

$$P_{pv} = V_{pv} \cdot I_{pv} = V_{pv} \cdot N_p \left(I_{ph} - I_{sat} \left[\exp \left(\frac{V_{pv}}{\gamma \cdot N_s} \right) - 1 \right] \right) \quad (6)$$

Then, the PV array's unidirectional step-up converter formulations [22] are considered as follows:

$$\begin{cases} \frac{dV_{pv}}{dt} = \frac{I_{pv}}{C_1} - \frac{I_{L-pv}}{C_1} \\ \frac{dI_{L-pv}}{dt} = f_1(x) + g_1(x) \cdot u_{pv} \\ \frac{dV_o}{dt} = f_2(x) + g_2(x) \cdot u_{pv} \end{cases} \quad (7)$$

where,

$$\begin{cases} f_1(x) = \frac{1}{L_{pv}} \left[V_{pv} + V_D - \frac{R \cdot R_c}{R+R_c} I_{L-pv} - \left(\frac{R_c}{R+R_c} - 1 \right) V_o \right] \\ g_1(x) = \frac{1}{L_{pv}} \left[V_D + \frac{R \cdot R_c}{R+R_c} I_{L-pv} - \left(\frac{R_c}{R+R_c} - 1 \right) V_o \right] \\ f_2(x) = \frac{1}{C} \left[\frac{R}{R+R_c} I_{L-pv} + \frac{1}{R+R_c} V_o \right] \\ g_2(x) = -\frac{R}{C(R+R_c)} I_{L-pv} \end{cases} \quad (8)$$

According to the expressions above, the DC link output voltage of the DC MG and the current value of the PV inductor are displayed as V_o and I_{L-pv} respectively, L_{pv} is the value of PV inductor, C depicts the capacitor value of the DC bus, $V_D = 0.82$ defines the diode voltage in a PV module which is associated with the voltage drop across the bypass diode during reverse bias conditions especially in scenarios where shading or low-light conditions, R illustrates the value of the resistive load and R_c corresponds to 39.6Ω . To create the desired PV or MPP voltage, the MPP section is developed according to the subsequent form [22]:

$$\frac{dP_{pv}}{dI_{pv}} = \frac{d(V_{pv} I_{pv})}{dI_{pv}} = V_{pv} + I_{pv} \frac{dV_{pv}}{dI_{pv}} = 0 \quad (9)$$

Considering (9) in light of (1), the PV voltage V_{pv} is achieved as the following expression:

$$V_{pv} = \gamma \cdot N_s \cdot \log \left(\frac{I_{sat} + I_{ph} - I_{pv}}{I_{sat}} \right) \quad (10)$$

The derivation result of the PV voltage V_{pv} concerning the PV current I_{pv} is depicted as follows:

$$\frac{dV_{pv}}{dI_{pv}} = -\gamma \cdot N_s \left(\frac{1}{I_{sat} + I_{ph} - I_{pv}} \right) \quad (11)$$

Replacing (10) and (11) in (9), the subsequent expression is achieved [22]:

$$\log \left(\frac{I_{sat} + I_{ph} - I_{pv}}{I_{sat}} \right) = \frac{1}{I_{sat} + I_{ph} - I_{pv}} \quad (12)$$

The expression that follows represents a relationship between the intended peak power current I_p and the photocurrent I_{ph} . This mathematical equation is an important tool for analyzing and optimizing solar systems. Maximizing power production is a key aim in the field of solar energy production, and this formula gives insights into how to achieve the objective.

$$I_p = 0.91 \cdot I_{ph} \quad (13)$$

Eventually, the needed desired value of the PV or MPP voltage V_{pv-ref} is produced [22] by substituting I_p with I_{pv} in (9):

$$V_{pv-ref} = \gamma \cdot N_s \cdot \log \left(\frac{I_{sat} + 0.09 \cdot I_{ph}}{I_{sat}} \right) \quad (14)$$

As the main role of the BSMC algorithm, it must force the PV voltage V_{pv} to track and match the desired PV voltage level V_{pv-ref} to achieve the peak power. The errors in the tracking of the PV voltage [22] and inductor current are illustrated as the following equations:

$$\begin{cases} e_1 = V_{pv} - V_{pv-ref} \\ e_2 = I_{L-pv} - I_{L-pv-ref} \end{cases} \quad (15)$$

where $I_{L-pv-ref}$ exhibits the desired inductor current, which will be described thereafter. Firstly, the time derivation result of the PV voltage error e_1 concerning (7) is achieved as the following expression [22]:

$$\dot{e}_1 = \frac{I_{pv}}{C_1} - \frac{I_{L-pv}}{C_1} - \dot{V}_{pv-ref} \quad (16)$$

The equation above is revised as the following expression:

$$\dot{e}_1 = \frac{I_{pv}}{C_1} - \frac{e_2}{C_1} - \frac{I_{L-pv-ref}}{C_1} - \dot{V}_{pv-ref} \quad (17)$$

In order to stabilize (17), the subsequent control expression is suggested as:

$$I_{L-pv-ref} = C_1 \left(\frac{I_{pv}}{C_1} - \dot{V}_{pv-ref} - M_1 \cdot e_1 - M_{1sw} \cdot \text{sign}(e_1) \right) \quad (18)$$

where M_1 and M_{1sw} are positive values and define the gains of the controller. Then, by introducing the Lyapunov candidate as $V_1 = \frac{1}{2} e_1^2$, one can be found:

$$\begin{aligned} \dot{V}_1 &= e_1 \cdot \dot{e}_1 = e_1 \left(\frac{I_{pv}}{C_1} - \frac{e_2}{C_1} - \frac{I_{L-pv-ref}}{C_1} - \dot{V}_{pv-ref} \right) \\ &= e_1 \left(-\frac{e_2}{C_1} - M_1 \cdot e_1 - M_{1sw} \cdot \text{sign}(e_1) \right) \\ &= -\frac{e_1 \cdot e_2}{C_1} - M_1 \cdot e_1^2 - M_{1sw} \cdot |e_1| \end{aligned} \quad (19)$$

Secondly, by taking derivative of $e_2 = I_{L-pv} - I_{L-pv-ref}$, one can be achieved:

$$\begin{aligned} \dot{e}_2 &= \dot{I}_{L-pv} - \dot{I}_{L-pv-ref} \\ &= f_1(x) + g_1(x) \cdot u_{pv} - \dot{I}_{L-pv-ref} \end{aligned} \quad (20)$$

The Lyapunov candidate function is selected as the following expression in order to stabilize (20):

$$V_2 = V_1 + \frac{1}{2} \cdot e_2^2 \quad (21)$$

By taking time derivative of the equation above and applying (19), one finds:

$$\begin{aligned} \dot{V}_2 &= -\frac{e_1 \cdot e_2}{C_1} - M_1 \cdot e_1^2 - M_{1sw} \cdot |e_1| + e_2 \cdot \dot{e}_2 \\ &= -\frac{e_1 \cdot e_2}{C_1} - M_1 \cdot e_1^2 - M_{1sw} \cdot |e_1| \\ &\quad + e_2(f_1(x) + g_1(x) \cdot u_{pv} - \dot{I}_{L-pv-ref}) \end{aligned} \quad (22)$$

Therefore, the subsequent regulation command is suggested:

$$u_{pv} = \frac{1}{g_1(x)} \left(-f_1(x) + \dot{I}_{L-pv-ref} + \frac{e_1}{C_1} - M_2 \cdot e_2 - M_{2sw} \cdot \text{sign}(e_2) \right) \quad (23)$$

where $M_2 > 0$ and $M_{2sw} > 0$ are the gains of the control method. The remainder of evidence is available in [23] for more detail.

3.2. SMC Current Control

The fuel cell as an additional power supply to help the PV system to properly meet the load demand is controlled by the SMC current controller. The sliding surface in the SMC strategy describes a situation in which the regulated current takes a specified path. The controller's goal is to drive actual current onto this sliding surface, guaranteeing that the fuel cell performs under the specified current level. The SMC strategy is robust against uncertainties, fluctuations in fuel cell properties, and disturbances from outside, making it suitable for practical uses characterized by changing and unforeseen circumstances. The proposed SMC current controller for regulating the fuel cell current is clearly illustrated in Fig. 3. Additionally, the SMC subsystem design is indicated as Fig. 4. Finally, the SMC parameters for this design are depicted in Table 2.

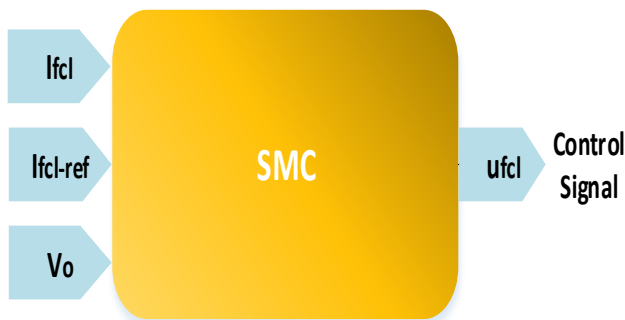


Fig. 3: SMC current controller

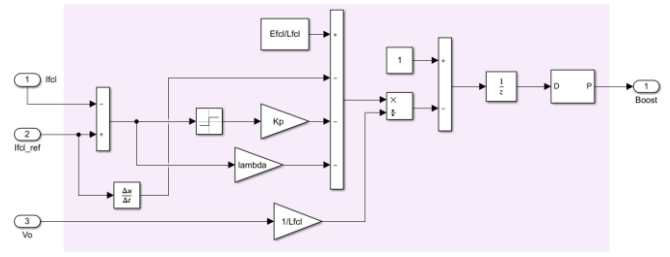


Fig. 4: SMC subsystem for fuel cell

$$\frac{dI_{fcl}}{dt} = -(1 - u_{fcl}) \frac{1}{L_{fcl}} V_o + \frac{V_{fcl}}{L_{fcl}} + d_{fcl} \quad (24)$$

where I_{fcl} , V_{fcl} and L_{fcl} are the fuel cell's voltage, current and inductance respectively. Moreover, the u_{fcl} represent the current control signal and d_{fcl} indicates the lumped uncertainty term for the unknown diode current of the fuel cell $I_{o_{fcl}}$ which assumed to be confined to:

$$|d_{fcl}(t)| \leq \Delta_{fcl} \quad (25)$$

where Δ_{fcl} defines the known positive constant. The error of the fuel cell current e_{fcl} is defined as the following expression:

$$e_{fcl} = I_{fcl} - I_{fcl-ref} \quad (26)$$

where $I_{fcl-ref}$ indicates the desired fuel cell current. By taking derivative of (26) and replacing (24), the following expression can be obtained:

$$\begin{aligned} \dot{e}_{fcl} &= \dot{I}_{fcl} - \dot{I}_{fcl-ref} \\ &= -(1 - u_{fcl}) \frac{1}{L_{fcl}} V_o + \frac{V_{fcl}}{L_{fcl}} + d_{fcl}(t) - \dot{I}_{fcl-ref} \end{aligned} \quad (27)$$

The subsequent control rule is suggested to stabilize the existing error dynamics (27):

$$u_{fcl} = 1 - \frac{L_{fcl}}{V_o} \left(\frac{V_{fcl}}{L_{fcl}} - \dot{I}_{fcl-ref} + K_{fcl} \cdot e_{fcl} + K_{fcl-sg} \cdot \text{sgn}(e_{fcl}) \right) \quad (28)$$

where K_{fcl} and K_{fcl-sg} are the control and the sliding gains respectively.

3.3. PI-SMC Voltage Control

An advanced control method known as PI-SMC has been presented to guarantee stable voltage control and efficient response to demand inside the DC MG. The overall configuration of this enhanced control method is clearly displayed in Fig. 5, highlighting the critical role it performs in improving the stability and functionality of the DC MG. Moreover, the SMC subsystem for this configuration is designed as Fig. 6. The SMC subsystem parameters are also demonstrated in Table 2. The PI regulator creates the desired battery current I_{b-ref} for the SMC by acquiring the

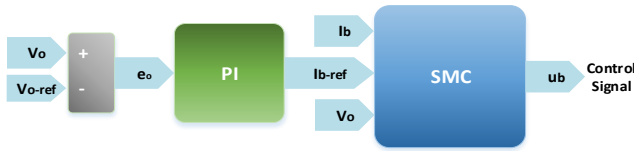


Fig. 5: PI-SMC voltage regulator

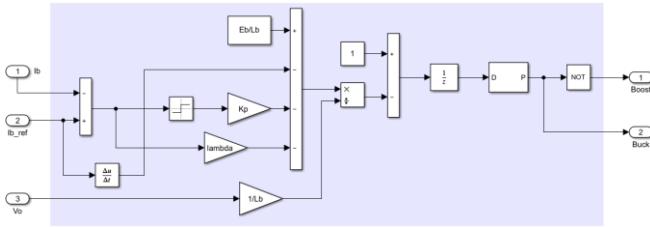


Fig. 6: SMC subsystem for BESS

Table 2: SMC subsystem parameters

Parameters	Values
Lithium-Ion battery nominal potential E_b	20 [V], 6.5 [Ah]
Fuel cell nominal voltage E_{fcl}	20[V]
Battery inductance L_b	3.3 [mH]
Fuel cell inductance L_{fcl}	3.3 [mH]
lambda	10
SMC constant K_p	100000

potential error between the reference DC link voltage V_{o-ref} and its actual value V_o . Then, the SMC block gets the BESS current I_b , the DC link voltage V_o , and the desired BESS current I_{b-ref} to maintain the DC link voltage V_o at the pre-defined voltage range, as well as manage the power sharing among the PV system, the fuel cell, and BESS to properly supply the fluctuating demanded power.

$$\begin{cases} \frac{dV_o}{dt} = \frac{1}{C} (1 - u_b) I_b + d_0(t) \\ \frac{dI_b}{dt} = -(1 - u_b) \frac{V_o}{L_b} + \frac{V_b}{L_b} + d_b(t) \end{cases} \quad (29)$$

where the BESS voltage is defined as V_b , the DC bus capacitance is indicated as C , and L_b shows the BESS inductor. Moreover, because the load current I_o and diode current of the BESS I_{o_b} are not known, the lumped parametric uncertainty terms of the output and the BESS are displayed as $d_0(t) = \frac{1}{C} (I_{opv} + I_{ofcl} - I_o)$ and $d_b(t)$, which supposed to be confined to:

$$\begin{cases} |d_0(t)| \leq \Delta_0 \\ |d_b(t)| \leq \Delta_b \end{cases} \quad (30)$$

where the noted positive fixed values are represented as Δ_0 and Δ_b . Defining the voltage and current tracking errors as the following expressions:

$$\begin{cases} e_o = V_o - V_{o-ref} \\ e_b = I_b - I_{b-ref} \end{cases} \quad (31)$$

The subsequent expression of the PI control method is used to generate the desired BESS current for the SMC approach.

$$I_{b-ref} = K_p \cdot e_o + K_i \cdot \int e_o dt \quad (32)$$

where the proportional and integral gains are represented as K_p and K_i . The time derivation result of the BESS current error e_b is obtained as the following formula:

$$\begin{aligned} \dot{e}_b &= \dot{I}_b - \dot{I}_{b-ref} \\ &= -(1 - u_b) \frac{V_o}{L_b} + \frac{V_b}{L_b} + d_b(t) - \dot{I}_{b-ref} \end{aligned} \quad (33)$$

Eventually, the following SMC concept is suggested to produce the control signal or duty cycle of the voltage tracking u_b as the following equation [24]:

$$u_b = 1 - \frac{L_b}{V_o} \left(\frac{V_b}{L_b} - \dot{I}_{b-ref} + K_b \cdot e_b + K_{b-sg} \cdot \text{sgn}(e_b) \right) \quad (34)$$

where the control and sliding gains of the BESS are indicated as K_b and K_{b-sg} respectively.

3.4. Stability Authentication

Lyapunov stability analysis is whether a dynamic system identified by a group of differential equations will develop toward a stable state or demonstrate instability over time. Introducing the Lyapunov function as the following equation:

$$V_{total} = V_2 + V_{fcl} + V_b = \frac{1}{2} \cdot e_2^2 + \frac{1}{2} \cdot e_{fcl}^2 + \frac{1}{2} \cdot e_b^2 \quad (35)$$

The following expression is resulted by taking derivative of (35) as follows:

$$\begin{aligned} \dot{V}_{total} &= -e_2^2 - e_{fcl}^2 - e_b^2 - S \cdot \dot{S} \\ &\leq -e_2^2 - e_{fcl}^2 - e_b^2 - \delta \cdot S^2 - \beta \cdot |S| \end{aligned} \quad (36)$$

Where $\dot{V}_{total} < 0$ as the result of positive δ and β . This specific derivative of the Lyapunov function assures that the system's paths go towards, instead of away from, the equilibrium point. This ensures that any fluctuation or disruption in the system will result in a return to stable condition.

4. SCENARIOS AND SIMULATION OUTCOMES

The proposed isolated DC MG and the proposed methodology are rigorously simulated in a software framework of MATLAB@R2020b/Simulink for result processing and to demonstrate the robust and effective functioning of the novel control structure. This simulation tool enabled comprehensive output analysis and verification of the control mechanism's effectiveness in a software-based setting. All simulations are performed on a 64-bit PC (Intel Core i5 CPU, 8G RAM, and Windows 7). Table 3 clearly summarizes the DC MG parameters, which are required for the simulation. This detailed simulation not only confirms the suggested control technique but also acts as a significant milestone in analyzing and assuring the most effective operation of the MG under different operating scenarios.

The PI-SMC control technique is proposed for the DC-DC buck-boost converter to reach the robust regulation of the DC link voltage and ensure an evenly distributed and efficient response to demand and input variations. The operating flowchart of the proposed control strategy is indicated as Fig. 7, in which P_{pv} , P_{fcl} , P_b and P_o demonstrate the output power of PV, fuel cell, BESS and load respectively. As depicted in this figure, if the total output power of the PV and fuel cell is larger than the output load power, the BESS switches to charging mode and the surplus power is stored in the BESS in order to maintain the balance between generation and consumption. Moreover, if the total supply of the PV and fuel cell is lower than the demanded output power, the BESS switches to discharging mode and the deficit supply power is provided by BESS. Finally, while the total generation amount meets the demanded load power, the BESS plays a pivotal role in offsetting losses within the MG. The proportional and integral parameters of the PI control method equal $K_p = 0.01$ and $K_i = 5$ respectively. A set of simulations containing shifts in both load demand and solar irradiation are undertaken to assess the effectiveness of the suggested controller, as depicted in Fig. 8 and, Fig. 9 respectively. These dynamic scenarios are intended to put the controller's capability to respond to changes in its operating conditions to the test. The output load varies inextricably with the needed load power, but variations in solar exposure have a direct influence on the generated PV power. To put it another way, the connection between the resistive load and asked load power is such that a rise in resistive load is equivalent to a drop in demanded load power. A reduction in the resistive load, on the other hand, indicates an increase in the requested power, establishing a direct relationship between load changes and the power requested by the system. In the meantime, changes in sun irradiance rates have an evident impact on the amount of PV production. As sun irradiance decreases, so does the output power of the PV system, resulting in a drop in produced PV power. All these changes on both the generation and consumption sides present dynamic difficulties to the system, increasing the tracking error of the DC MG output voltage e_o and threatening voltage stability. The interaction between variations in solar irradiance and load demand has an immediate effect on the DC link voltage balance, rendering it subject to swings that might jeopardize the whole system's stability. The suggested nonlinear robust controller's capability is well demonstrated in Fig. 10, displaying its extraordinary ability to preserve the DC link voltage at the desired level of 50 V in a variety of challenging scenarios, such as different load demands and sun exposure amounts, which lead to potential voltage drops and spikes. Significantly, the control unit has an outstanding capability to suppress voltage drops and spikes and retain the DC bus voltage with minimal fluctuations and at a high-speed rate. Additionally, the efficient demand response among the PV, fuel cell and BESS to supply the requested demand is fulfilled as indicated in Fig. 11 considering the subsequent scenarios. Fig. 12 and Fig. 13 also display the output load current and the output load power respectively, which are changed by the declared step variations.

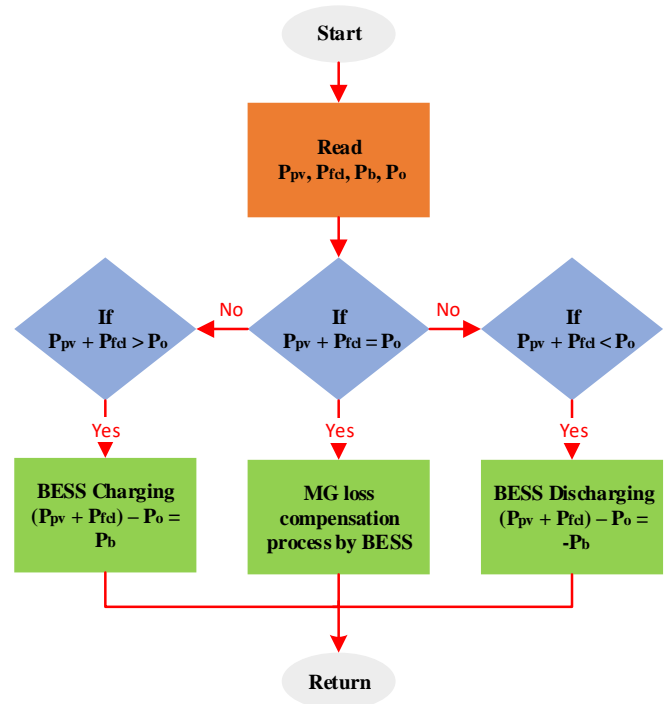


Fig. 7: Flowchart of BESS PI-SMC Controller

4.1. Scenario 1: An Increase in Demand ($2 < t < 4$)

In this case, a decrease in resistive load to 6.25Ω is followed by a rise in necessary load power, which now reaches 400 W. As a result, the BESS must switch smoothly into discharging mode to augment total power production and satisfy the increased load power requirement. This operational adjustment is necessary because the total power produced by the PV system and the fuel cell is inadequate to meet the increased load power need. The BESS successfully provides more power to compensate for the shortage by discharging, guaranteeing the total delivered power corresponds with the increasing load demand.

4.2. Scenario 2: A Decrease in Demand ($6 < t < 8$)

In this scenario, a fall in required load power to 200 W is accompanied by a rise in resistive load to 12.5Ω . This modification causes a change in the power sharing approach, in which the generation units, which include the PV system and the fuel cell, successfully meet the required power demand. As a result, the excess power produced during this time is smartly routed to the BESS for storage. This crucial management guarantees that the power provided by the generation units meets the decreased load power demand and facilitates surplus energy storage in the BESS.

4.3. Scenario 3: No Change in Demand

Since the required output demand is exactly aligned with the total power generation of the PV system and the fuel cell, which equals 300 W, the BESS is not used for demand support. At a resistive load rating of 8.33Ω , this balance between demanded and produced power eliminates the need for BESS involvement in satisfying the load demand. Instead, the BESS is critical in meeting the MG losses, guaranteeing the whole system functions at peak efficiency and in balance.

Table 3: DC MG parameters

Parameters	Values
DC bus capacitance C	1000 [μ F]
PV capacitance C_1	1000 [μ F]
PV inductor L_{pv}	1.21 [mH]
Battery inductance L_b	3.3 [mH]
Fuel cell output power P_{fcl}	100 [W]
Switching frequency f_s	50 [kHz]
Load powers P_o	400, 300, 200 [W]
Variable resistive load values R_{Load}	6.25, 8.33, 12.5 [Ω]

4.4. Scenario 4: A Decrease in Irradiance ($10 < t < 12$)

The sun irradiation is reduced to 500 W/m^2 during this specific time frame. As a result, the produced power from the PV system drops to around 100 W. In reaction to the decrease in PV power production, and in order to maintain an uninterrupted power supply to satisfy the requested load demand, the BESS quickly changes to discharging mode again. By switching to this mode, the BESS compensates for the reduced PV power by giving the required power to meet the load requirement. In addition to deal with voltage drops and spikes due to shifts in supply and demand, and preserve the DC link voltage at the reference voltage level, as the main goal of the research, to maintain the overall stability of the MG's system, the novel MPP-based BSMC technique is presented as a unique method for the DC-DC step-up converter in the PV system. The fundamental goal of this strategy is to effectively maximize the power production from the PV panels by tracking the MPP as effectively as possible. This critical work is depicted in Fig. 14, where it is clear that the suggested technique allows the PV output voltage V_{pv} to swiftly match its desired value or the MPP voltage V_{pv-ref} which equals 26.6 V. Moreover, the PV output current equals almost 7.55 A as indicated in Fig. 15. Thus, the derived peak power arrives at 200 W in solar exposure amount of 1000 W/m^2 and the cell temperature of 25°C as illustrated in Fig. 16. It's also worth noting that the suggested MPP-based BSMC method is intended to solve the unpredictable behavior of solar irradiation levels. In practice, the quantity of solar irradiation falling on the PV panels can vary fast, as illustrated by a change from 1000 W/m^2 to 500 W/m^2 at $10 < t < 12$ in Fig. 9. In reaction to such shift, the MPPT controller expertly modifies the PV array's operation point, allowing for maximum energy harvesting under variable irradiance circumstances. Fig. 17, Fig. 18 and Fig. 19 clearly point out the BESS voltage, output power and current respectively, in which the BESS charging and discharging modes are visible. As demonstrated in Fig. 19, the magnitude of the BESS current equals to 5 A. The sign of the current is positive and negative for BESS discharging and charging modes respectively. As a result, the multiplication of the BESS current and voltage represent the BESS discharging and charging output power as represented in Fig. 18. Finally, the output current and power of the fuel cell are indicated in Fig. 20 and Fig. 21 respectively.

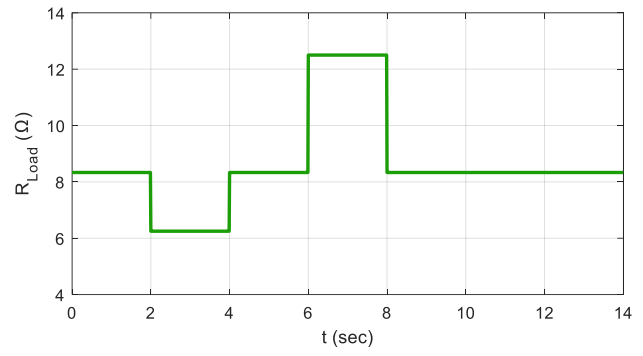


Fig. 8: Step changes in load

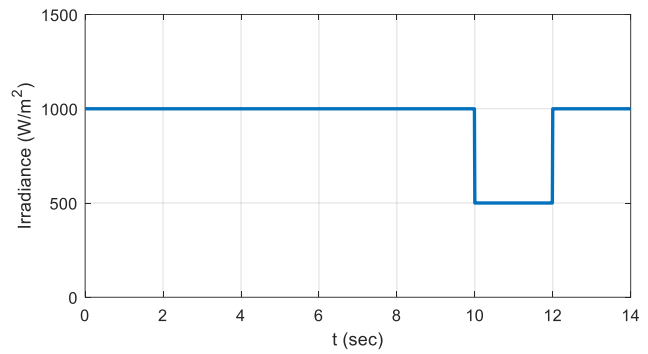


Fig. 9: Step change in solar irradiation

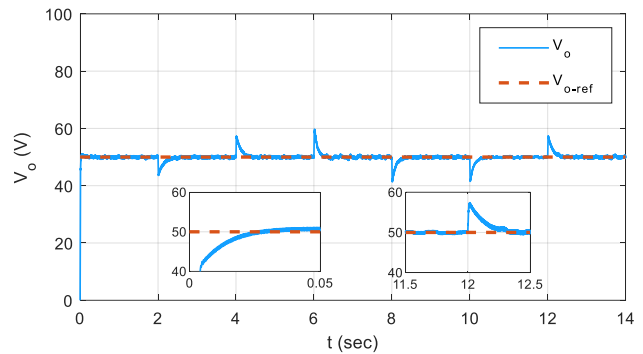


Fig. 10: DC bus voltage

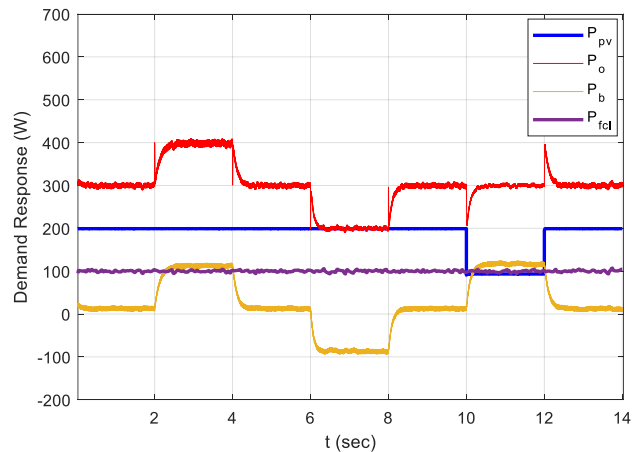


Fig. 11: Efficient balanced demand response

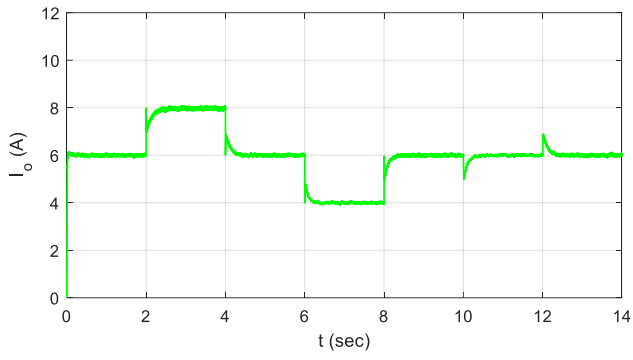


Fig. 12: Load current

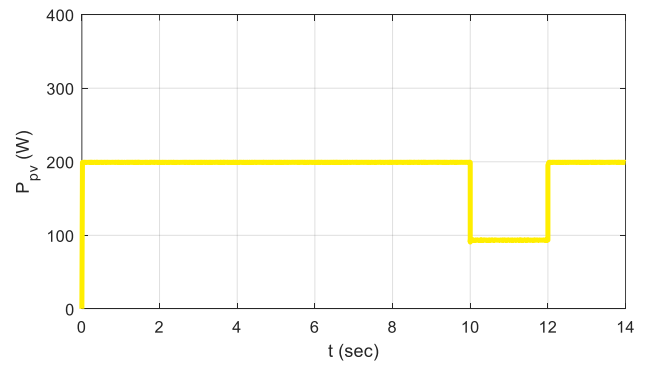


Fig. 16: PV output power

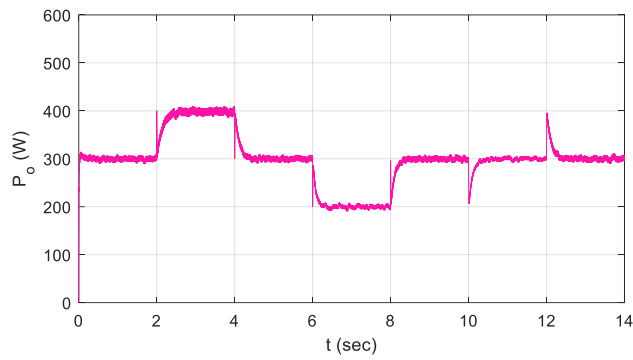


Fig. 13: Demand load power

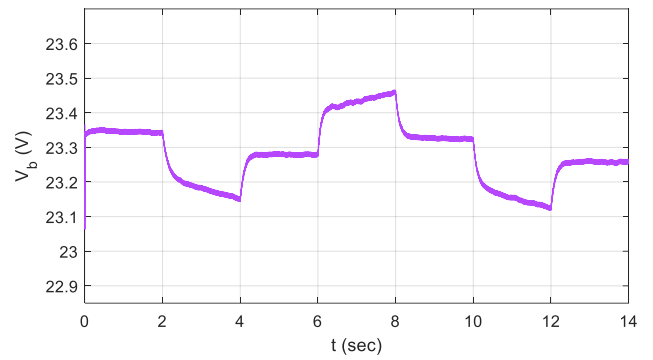


Fig. 17: BESS voltage

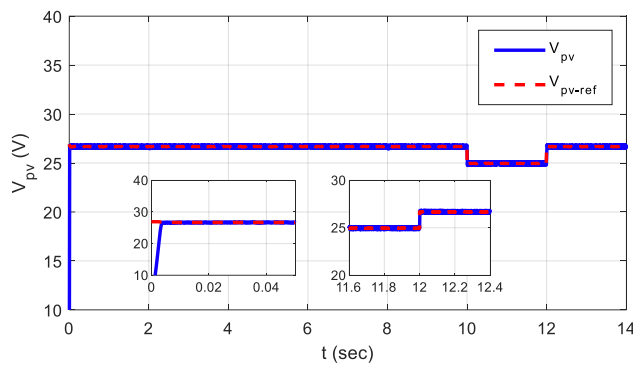


Fig. 14: PV voltage

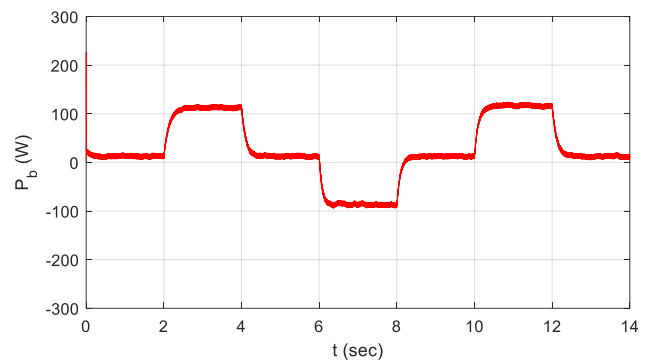


Fig. 18: BESS output power

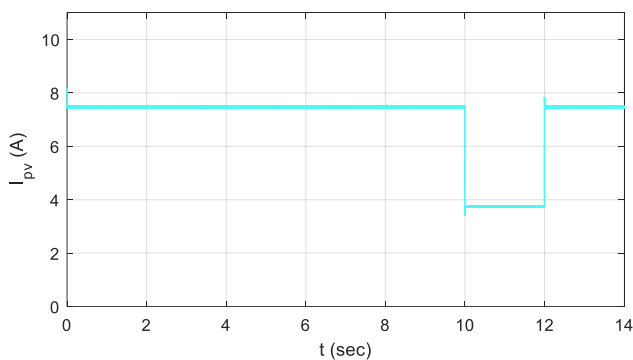


Fig. 15: PV current

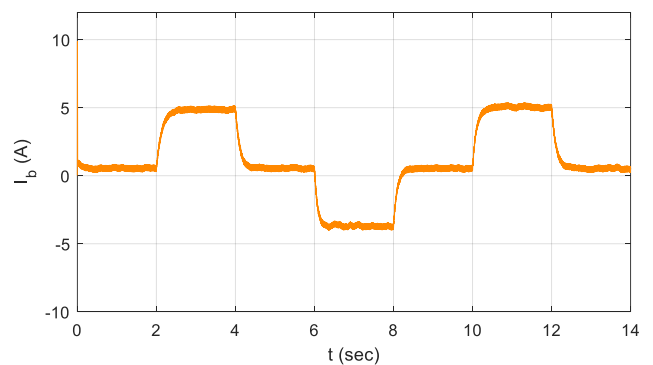


Fig. 19: BESS current

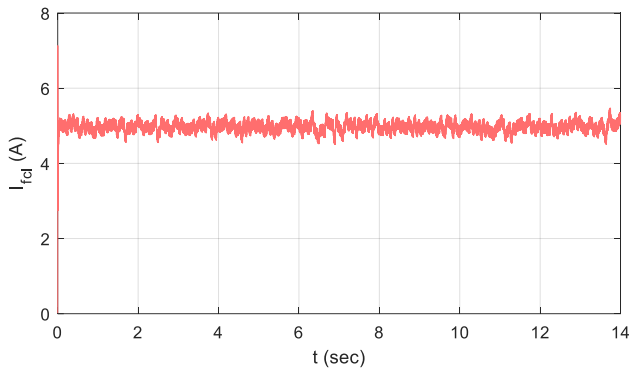


Fig. 20: Fuel cell current

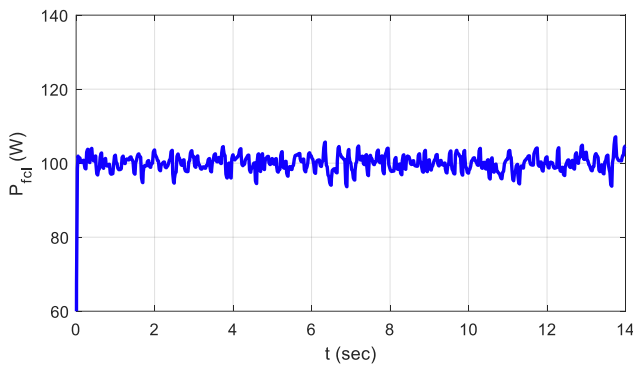


Fig. 21: Fuel cell output power

5. CONCLUSION

In the face of fluctuating load and varying sun radiation exposures, this research developed a robust PI-SMC as a nonlinear cascaded controller for voltage control and efficient response to demand of a freestanding DC MG comprising of PV, BESS, and fuel cell. In order to successfully reach the MPP and extract the highest feasible output from the solar array, an MPP-based BSMC technique is additionally proposed and examined. Furthermore, BESS is becoming accessible to aid in the power distribution of the PV system and fuel cell. The suggested control approach fulfills the charging and discharging process of the BESS to react to the changing demanded power and save the extra power. The functionality of the proposed control method is demonstrated by modelling the DC MG under demand changes and varied solar irradiations. This technique ensures efficient and robust control of the DC link voltage with extremely tiny variations and rapid response. This model is also applicable over extended time frames and for consumers with larger demand through installing extra PV modules and taking into account the precise power sharing among the PV system, the BESS, and the fuel cell. Furthermore, the devised regulating approach is simple to adopt and ensures system stability. In regard to significance, this study contributes to the development of DC MG control approaches by providing a straightforward yet efficient and robust control method. Future studies could focus on numerical comparisons with current benchmark and as well as prior efforts to evaluate the proposed methodology's effectiveness.

CREDIT AUTHORSHIP CONTRIBUTION STATEMENT

Sajed Derakhshani Pour: Funding acquisition, Project administration, Supervision, Validation. **Reza Eslami:** Conceptualization, Data curation, Formal analysis, Investigation, Methodology, Resources, Software, Visualization, Roles/Writing - original draft, Writing - review & editing.

DECLARATION OF COMPETING INTEREST

The authors declare that they have no known competing financial interests or personal relationships that could have appeared to influence the work reported in this paper. The ethical issues; including plagiarism, informed consent, misconduct, data fabrication and/or falsification, double publication and/or submission, redundancy has been completely observed by the authors.

REFERENCES

- [1] P. Singh and J. S. Lather, "Dynamic current sharing, voltage and SOC regulation for HESS based DC microgrid using CPISM technique," *Journal of Energy Storage*, vol. 30, p. 101509, 2020.
- [2] V. Suresh, N. Pachauri and T. Vigneysh, "Decentralized control strategy for fuel cell/PV/BESS based microgrid using modified fractional order PI controller," *International Journal of Hydrogen Energy*, vol. 46, no. 5, pp. 4417-4436, 2021.
- [3] A. Dimovski, M. Moncecchi and M. Merlo, "Impact of energy communities on the distribution network: An Italian case study," *Sustainable Energy, Grids and Networks*, vol. 35, p. 101148, 2023.
- [4] S. A. Mehraban and R. Eslami, "Multi-microgrids energy management in power transmission mode considering different uncertainties," *Electric Power Systems Research*, vol. 216, p. 109071, 2023.
- [5] M. Tofighi-Milani, S. Fattaheian-Dehkordi and M. Fotuhi-Firuzabad, "A New Peer-to-Peer Energy Trading Model in an Isolated Multi-agent Microgrid," *Journal of Applied Research in Electrical Engineering*, vol. 1, no. 1, pp. 33-41, 2022.
- [6] A. M. Dezfuli, M. Abasi, M. E. Hasanzadeh and M. Joorabian, "Voltage and Frequency Control Considering Disturbance in Input Power of DG," *Journal of Applied Science in Electrical Engineering*, *Journal of Applied Science in Electrical Engineering*, 2024.
- [7] B. Modu, M. P. Abdullah, M. A. Sanusi and M. F. Hamza, "DC-based microgrid: Topologies, control schemes, and implementations," *Alexandria Engineering Journal*, vol. 70, pp. 61-92, 2023.
- [8] S. Vasantharaj, V. Indragandhi, V. Subramaniaswamy, Y. Teekaraman, R. Kuppasamy and S. Nikolovski, "Efficient Control of DC Microgrid with Hybrid PV—Fuel Cell and Energy Storage Systems," *Energies*, vol. 14, no. 11, p. 3234, 2021.
- [9] M. Shirkhani, J. Tavoosi, S. Danyali, A. Khosravi Sarvenoe, A. Abdali, A. Mohammadzadeh and C. Zhang, "A review on microgrid decentralized energy/voltage control structures and methods," *Energy Reports*, vol. 10, pp. 368-380, 2023.

- [10] Z. Lu, L. Wang and P. Wang, "Review of Voltage Control Strategies for DC Microgrids," *Energies*, vol. 16, no. 17, p. 6158, 2023.
- [11] R. Kumar and M. K. Pathak, "Distributed droop control of dc microgrid for improved voltage regulation and current sharing," *IET Renewable Power Generation*, vol. 14, no. 13, pp. 2499-2506, 2020.
- [12] Y. Liu, W. Deng, P. Yang, Y. Teng, X. Zhang, Y. Yang and W. Pei, "Dispatchable Droop Control Strategy for DC Microgrid," *Energy Reports*, vol. 9, pp. 98-102, 2023.
- [13] B. Li, C. Yu, X. Lu and F. Wang, "A novel adaptive droop control strategy for SoC balance in PV-based DC microgrids," *ISA Transactions*, vol. 141, pp. 351-364, 2023.
- [14] K. Ahmed, I. Hussain, M. Seyedmahmoudian, A. Stojcevski and S. Mekhilef, "Voltage Stability and Power Sharing Control of Distributed Generation Units in DC Microgrids," *Energies*, vol. 16, no. 20, p. 7038, 2023.
- [15] N. G. and J. K., "Real-time implementation of sliding mode controller for standalone microgrid systems for voltage and frequency stabilization," *Energy Reports*, vol. 10, pp. 768-792, 2023.
- [16] D. Sattianadan, G. R. P. Kumar, R. Sridhar, K. V. Reddy, B. S. U. Reddy and P. Mamatha, "Investigation of low voltage DC microgrid using sliding mode control," *International Journal of Power Electronics and Drive Systems*, vol. 11, no. 4, pp. 2030-2037, 2020.
- [17] S. Y. Rahme, S. Islam, S. M. Amrr, A. Iqbal, I. Khan and M. Marzband, "Adaptive sliding mode control for instability compensation in DC microgrids due to EV charging infrastructure," *Sustainable Energy, Grids and Networks*, vol. 35, p. 101119, 2023.
- [18] S. Patel, A. Ghosh and P. K. Ray, "Efficient power management and control of DC microgrid with supercapacitor-battery storage systems," *Journal of Energy Storage*, vol. 73, p. 109082, 2023.
- [19] A. N. Akpolat, M. R. Habibi, E. Dursun, A. E. Kuzucuoğlu, Y. Yang, T. Dragičević and F. Blaabjerg, "Sensorless Control of DC Microgrid Based on Artificial Intelligence," *IEEE Transactions on Energy Conversion*, vol. 36, no. 3, pp. 2319-2329, 2021.
- [20] Z. Karami, Q. Shafiee, Y. Khayat, M. Yaribeygi, T. Dragičević and H. Bevrani, "Decentralized Model Predictive Control of DC Microgrids With Constant Power Load," *IEEE Journal of Emerging and Selected Topics in Power Electronics*, vol. 9, no. 1, pp. 451-460, 2021.
- [21] Q. Guo, I. Bahri, D. Diallo and E. Berthelot, "Model predictive control and linear control of DC-DC boost converter in low voltage DC microgrid: An experimental comparative study," *Control Engineering Practice*, vol. 131, p. 105387, 2023.
- [22] K. Dahech, M. Allouche, T. Damak and F. Tadeo, "Backstepping sliding mode control for maximum power point tracking of a photovoltaic system," *Electric Power Systems Research*, vol. 143, pp. 182-188, 2017.
- [23] S. Shoja-Majidabad and A. Yazdani, "Paralleled DC-DC Converters Control Using Master-Slave Adaptive Fuzzy Backstepping Techniques," *Iranian Journal of Science and Technology, Transactions of Electrical Engineering*, vol. 45, pp. 1343-1367, 2021.
- [24] S. Shoja-Majidabad and S. D. Pour, "Robust control of multi-phase interleaved boost converters in the presence of perturbations and open phase fault," *International Journal of Power Electronics*, vol. 16, no. 2, pp. 162-179, 2022.

BIOGRAPHY



Sajed Derakhshani Pour received the B.Sc. in Electrical Engineering from the Department of Electrical Engineering, University of Bonab, Bonab, Iran, in 2020, and he is currently studying M.Sc. in Sustainable Smart Grids for Energy Transition (R2E) at the Department of Energy, Polytechnic University of Milan, Milan, Italy, since 2022. His research interests oriented to renewable energy systems, energy storage systems and smart/micro grids.



Reza Eslami received the B.Sc., M.Sc. and Ph.D. degrees in Electrical and Electronics Engineering from the Department of Electrical Engineering, Amirkabir University of Technology, Tehran, Iran, in 2010, 2012 and 2017 respectively. He has also worked as an Associate Professor with the Department of Electrical Engineering, Sahand University of Technology, Tabriz, Iran, since 2017. His research interests are smart grids and power system protection.

Copyrights

© 2024 by the author(s). Licensee Shahid Chamran University of Ahvaz, Ahvaz, Iran. This article is an open-access article distributed under the terms and conditions of the Creative Commons Attribution –NonCommercial 4.0 International (CC BY-NC 4.0) License (<http://creativecommons.org/licenses/by-nc/4.0/>).

